Original Article
Molecular and functional characterization of non voltage-operated Ca²⁺ entry in gastrointestinal neuroendocrine tumor cells

Sasi Arunachalam*, Tetyana Zhelay*, David R. Giovannucci

Department of Neurosciences, University of Toledo College of Medicine, Toledo OH 43614, USA.

*Contributed equally and should be considered co-primary authors.

Abstract: Ca^{2+} entry through non-voltage operated channels serves as a key signaling component for tumor progression in a variety of cancers including prostate, colon and breast. As a starting point for an inquiry into the role of Ca^{2+} signaling pathways in gastroenteropancreatic neuroendocrine cancers, including carcinoid, we characterized Ca^{2+} entry in a set of human carcinoid cell lines originating in the foregut, midgut and hindgut. In the current study, we provide molecular and functional evidence for store-operated and other non-voltage operated Ca^{2+} permeable channels in carcinoid tumor cell lines. RT-PCR technique was used to profile an array of non voltage-operated Ca^{2+} channels in carcinoid cell lines. Live-cell imaging methods were used to functionally assess store operated Ca^{2+} entry (SOCE) following depletion of ER Ca^{2+} stores by cyclopiazonic acid. Treatment with pharmacological inhibitors of SOCE generally reduced Ca^{2+} entry. We also demonstrated that SOCE in some carcinoid cell lines was activated by neurotransmitter suggesting that Ca^{2+} entry through specific channels may be important for mediating neural, paracrine or autocrine signals in the gut in health and disease such as carcinoid cancer.

Keywords: Store-operated, Orai, STIM, TRP, fura-2, carcinoid

Introduction

The spatial and temporal dynamics of cytosolic calcium levels provide critical regulatory control over a vast array of cellular processes [1] [2]. For example, in both non-transformed and transformed cell types growth factors evoke Ca^{2+} oscillations that can promote reentry into the cell cycle, migration and invasive activity. Typically, the maintenance of oscillations is dependent not only on Ca^{2+} release from internal stores but on Ca^{2+} entry as well. Prolonged Ca^{2+} entry can activate a number of signaling pathways including cell proliferation and has been shown to regulate transcription factors like NFAT and CREB [3]. Thus, signal specificity is largely dependent on the generation of signature patterns of cytosolic Ca^{2+} changes. Often those changes are compartmentalized with their downstream effectors [4]. Given the ubiquitous role of Ca^{2+} as second messenger, it is not sur-

prising that Ca^{2+} channels resident in both intracellular organelles and plasma membrane have been implicated in a variety of disease states, including cancer [5]. Recent work by a few labs has focused on the role of Ca^{2+} permeable ion channels that mediate store-operated Ca^{2+} entry (SOCE) as a signal for transcriptional regulation, cell growth and survival in metastatic cells including breast, colon and prostate cancers [6-8].

In the current study molecular and functional approaches were used to profile SOCE in a heterogeneous set of uncommon tumors referred to collectively as gastroenteropancreatic neuroendocrine tumors (GEPNETs). These tumors are generally comprised of cells that exhibit both epithelial and neuronal features. This is the case for malignant cells with enteroendocrine or enterochromaffin phenotype often called carcinoid and believed to arise from cells of the dif-

Table 1. Cell lines

Cell line	Origin	Metastatic	Features	References
BON	Foregut (pancreas)	Yes	Secretes serotonin (5-HT), Neurotensin, Pancreastatin, Chromogranin A, Bombesin.	Ann N Y Acad Sci 2004;1014:179-88. Gastroenterology 2001;121:1400-6. Pancreas. 1994;9:83-90
H727	Foregut (lung)	Not definitive	PTH-like protein (PLP) secretion	Endocrinology. 1991;128(6):2999-3004
CNDT2.5	Midgut (ileum)	Yes	Secretes serotonin (5-HT) Expresses IGFR, PDGFR, EGFR, cMET, VGFR and SSTR1 - SSTR5.	Clin Cancer Res. 2007;15;13:4704-12
HC45	Midgut (ileum)	Yes	Express TGFßR (CgA, Band 7B2), EGFR receptor, and SSTR	Endocr Pathol 2007;18:223–2
HC49	Hindgut (rectum)	Yes	Expresses TGFßR, (CgA, band 7B2), EGFR and SSTR	Endocr Pathol (2007) 18:223–232

fuse neuroendocrine system of the GI tract [9-11]. Although carcinoid cancer cells have been shown to express voltage-operated Ca^{2+} channels (VOCCs) that mediate the secretion of peptides and biogenic amines that contribute to carcinoid syndrome and crisis, the role of SOCE in secretory function or in the development, maintenance or progression of GEPNETs such as carcinoid is largely unknown. Because there are few treatment options available for patients with inoperable tumors it is important to identify potential new diagnostic and therapeutic targets.

We now address whether store-operated Ca^{2+} channels are expressed and function in a set of human carcinoid cell lines originating from the foregut, midgut and hindgut. The molecular and functional profiling presented in this study provides further clarification of the routes of Ca^{2+} entry in enteroendocrine cells in health and disease.

Materials and methods

Cell culture

A variety of human foregut, midgut and hindgut carcinoid cell lines were used for the current study (**Table 1**). The foregut carcinoid cell line, BON originally derived from a carcinoid tumor metastatic to the pancreas was grown in Dulbecco's Modified Essential Medium (DMEM) supplemented with 10% FBS. The bronchial carcinoid cell line H727 was grown in RPMI with L-glutamine and supplemented with 10% FBS, 1% sodium pyruvate (100 mM) and 1% HEPES (1 M). HC45 and HC49 cell lines originally de-

rived from human ileal and rectal carcinoids, respectively were grown in RPMI with L-glutamine supplemented with 10% FBS, 5% horse serum and 1μg/mL of insulin. Another ileal carcinoid cell line, CNDT2.5 was maintained in DMEM supplemented with 10% FBS and 1% sodium pyruvate and 1% HEPES. All the cell lines were maintained at 37 °C in a humidified incubator set at 5% CO$_2$. The cell lines were harvested following brief treatment with Trypsin/EDTA (0.25%). All cell lines were passaged at the ratios recommended by provider. BON cells were provided by Dr. Kjell Oberg, Uppsala Sweden. H727 cells were purchased from American Type Culture Collection (ATCC). Human ileal and rectal carcinoid cell lines derived from liver metastases, HC45 and HC49 cells, respectively were gifts of Dr. Ricardo Lloyd, Mayo Clinic Rochester, MN. The ileal carcinoid line CNDT2.5 was provided by Dr. Lee Ellis, M.D. Anderson Cancer Center, Houston, TX.

Live cell imaging

For live cell imaging experiments, cells were plated on clean glass coverslips that were used to form the bottom of a recording chamber. Changes in cytosolic Ca^{2+} levels were monitored using fura-2 fluorescence method. For loading with fura-2 AM, cells were incubated with physiological saline solution (containing 140 mM NaCl, 5 mM KCl, 2.2 mM CaCl$_2$, 1 mM MgCl$_2$, 10 mM HEPES, and 5 mM glucose, pH 7.35) containing 2 μM fura-2 AM for 30-40 min at 25°C. Following loading protocol, cells were mounted on the stage of an Olympus IX-71 microscope equipped with a 40X oil-immersion objective (NA = 1.4). An air pressure driven de-

Table 2. Primers

Gene	Accession No.	Primer sequence	Product (BP)
Orai1	NM_032790	F:AGTTACTCCGAGGTGATGAGCC R:GACCGAGTTGAGATTGTGCAC	306
Orai2	NM_032831	F:ATGAGTGCTGAGCTTAACGTG R:GACTCGCTGATGGAGTTCAG	410
Orai3	BC006126	F:CCACATTGAAGCTGTGAGCA R:CAGGCGATTCAGTTCCTCTA	502
STIM1	NM_003156	F:AGCTCATCAGCGTGGAGGAC R:CCTTGAGGTGATTATGGCGAGT	300
TRPC1	NM_003304	F:GACTCTGGTATGAAGGGTTGGA R:CATACAGTTGTGTCAGTCCAATTG	357
TRPC3	U47050	F:CTTCTCTAGGTCCATGGAGGGAA R:TCAGAGTGAGACGCTTGCTGGC	419
TRPC4	AF063822	F:CTCTGGTTGTTCTACTCAACATG R:CCTGTTGACGAGCAACTTCTTCT	804
TRPC5	NM_012471	F:GTCGTGGAATGGATGATATTG R:GTTAGGCTCATCGATAGCTCTG	450
TRPC6	AJ006276	F:GAACTTAGCAATGAACTGGCAGT R:CATATCATGCCTATTACCCAGGA	626
TRPC7	NM_020389	F:ACTTCTATGCCTACGACGAGGAC R:CTAGTCTGGCTAACTCGTTGCTG	309
TRPV5	NM_019841	F:GGCCTATGAGACACGTGAAGATATC R:ATAGAATTGCCCCAGACTGGTTG	448
TRPV6	NM_018646	F:AGCCTACATGACCCCTAAGGACG R:GTAGAAGTGGCCTAGCTCCTCGG	448
TRPM5	NM_014555	F:GCTTCTTCACAGACGAGGA R:AGTCCTCCAGCAGCAGTG	471
TRPM6	NM_024080	F:GACCTGTGGAATGTGATGGA R:CAGCAGGATGTTGGTGGAT	528

vice was used to exchange physiological saline or solutions containing agonists or antagonists by local application through a glass capillary placed at the edge of the field of view. Cells were alternately illuminated at 340 and 380 nm light focused using a fiber optic guide and epifluorescence condenser onto the image plane by dichroic mirror (Semrock) using a monochromator-based Polychrome IV imaging system (TILL Photonics) and emission was detected using 510 nm ± 25 nm band pass filter (Semrock) and IMAGO QE camera. Changes in intracellular calcium were represented by and expressed as the ratio of fura-2 fluorescence (F340/F380).

Ca^{2+} entry measurements by Mn^{2+} quenching of fura-2 fluorescence

Cells were loaded with fura-2 AM as described in the preceding section. Following CCh or CPA treatment to induce a reduction in ER Ca^{2+} content, Mn^{2+}, which is known to bind to fura-2 with very high affinity and to strongly quench its fluo-

rescence was added at a concentration of 1 mM to the bath solution. The rate of Mn^{2+} quenching of the fura-2 fluorescence signal at the Ca^{2+} insensitive isosbestic excitation wavelength (360 nm) was determined and used as a semi-quantitaive indicator of plasma membrane mediated Ca^{2+} entry.

RT-PCR profiling

Carcinoid cell lines were trypsinized at 75-90% confluency and mRNA were extracted using Qiagen RNeasy as described by the manufacturer. Extracted RNA was reverse transcribed to cDNA using SuperScript II RT (Invitrogen) and used as template for identifying candidate genes. Specific primer sets were designed using Primer3 software (http://fokker.wi.mit.edu/primer3/input.htm) unless otherwise noted and were synthesized by Integrated DNA Technologies. Primers selected (**Table 2**) were made with the following parameters: length between 18-27 bases, T$_m$ between 53°-63°C, and primer GC%

between 20-80%. The web-based Blast program (available at the NCBI website) was used to determine specificity of the sequences.

The PCR reactions using specific primers were carried out using Platinum® Taq DNA polymerase (Invitrogen) under the following conditions: denaturing at 95°C for 30 s, annealing at 53°C for 30 s, and primer extending at 72°C for 30 s for 30 cycles. PCR products were separated by electrophoresis (120 V for 50-60 minutes) on a 1.5% agarose gel stained with ethidium bromide and sizes determined using a 50 bp DNA ladder. For each cell line/experiment, actin signal was used to normalize to relative levels

Results

Identification of non voltage-operated Ca^{2+} entry pathways by RT-PCR

In contrast to our understanding of the molecular underpinnings of HVA currents and voltage-operated Ca^{2+} entry in excitable cells, the channels involved in Ca^{2+} entry in non-excitable cells are less well-defined and very little is known about non voltage-operated Ca^{2+} entry pathways in carcinoid cell lines. Over the last decade a great many candidate channel proteins have been identified and proposed to underlie two major forms of Ca^{2+} entry in non-excitable cells: store-operated Ca^{2+} entry (SOCE) and store-independent, receptor operated Ca^{2+} entry (ROCE) [12]. SOCE is induced by the depletion of ER Ca^{2+} stores following intracellular Ca^{2+} channel activation. Until recently, the retrograde signal that activates SOCE was not well understood and has been the subject of intense study for many years. ROCE is activated by ligand-mediated or plasma membrane-delimited signals and is independent of store-depletion. Both SOCE and ROCE have been implicated in regulating cell growth and migration characteristics in prostate [8, 13] and colon cancer [6, 7, 14]. We therefore undertook experiments to identify various potential candidates for non voltage-operated Ca^{2+} entry in carcinoid cell lines. Semi-quantitative conventional endpoint RT-PCR was used to screen carcinoid cell lines for an array of non voltage-operated channel transcripts. Products were identified based on predicted base pair size and band signal intensity was normalized to ß-actin gene expression levels. RT-PCR results are summarized in **Figure 1**. Some
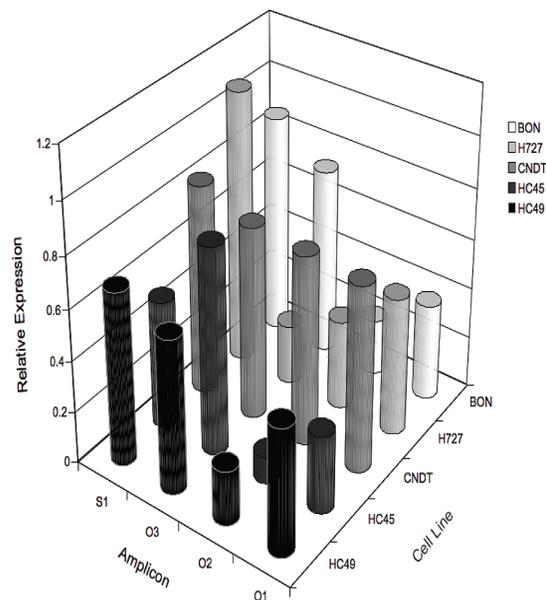
Figure 1. Semi-quantitative endpoint RT-PCR identifying transcripts for the pore forming channel proteins Orai 1-3 and the Ca^{2+} sensor STIM1 in a set of carcinoid cell lines. Multimeric assemblies of Orai and STIM proteins are believed to form a store-operated Ca^{2+} permeable channel. Gel band signal intensities were determined by densitometry and normalized to ß-actin expression levels. Mean ratio values represent result of at least independent 3 experiments.

of channel transcripts identified in the carcinoid cell lines tested have been implicated as likely candidate proteins that underlie SOCE [15]. For example, we found that STIM, Orai1-3 and TRPC1 transcripts were robustly expressed in all of the carcinoid lines tested. Of these the co-expression of STIM and Orai1 was shown by others to recapitulate many of the functional features of SOCE.

In addition to STIM and Orai, other non-VOCC transcripts were differentially expressed in carcinoid cell lines as shown in **Figure 2**. In these experiments we focused on the canonical TRP protein family, and on the Ca^{2+}-selective TRPV5 and TRPV6 channels that are expressed in the intestinal mucosa. Although there is evidence that some of these channels may contribute to SOCE in a tissue specific manner, TRP channel activation in many cases appears independent of store depletion.

TRPC1 was strongly expressed in all the cell
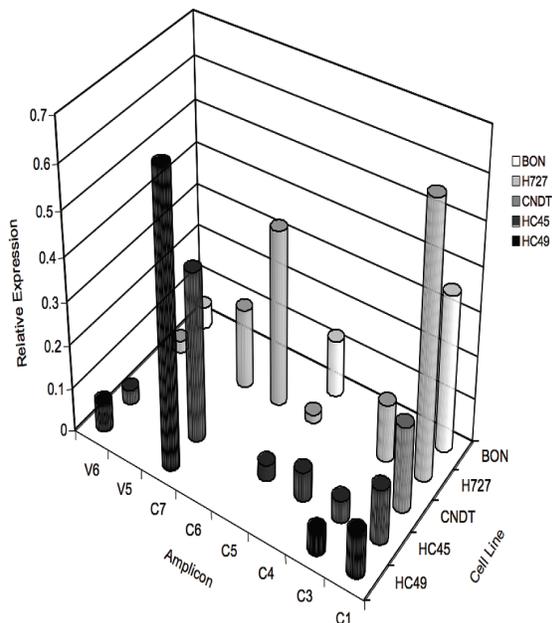
Figure 2. Semi-quantitative RT-PCR identifying some TRPC and TRPV transcripts in carcinoid cell lines. These channels are non-selective or highly selective for Ca^{2+} respectively, and are generally thought to play sensory roles in a variety of cell types. In addition some TRP channels have been proposed to SOCE in some cell types. Gel band signal intensities were determined as in Figure 1.

lines tested. In contrast, transcripts for TRPC3-7 were differentially expressed among the various carcinoid cell lines. TRPC6 was exclusively identified in H727; TRPC7 was expressed in all carcinoid lines except BON; and TRPC5 was expressed in all carcinoid lines but absent in hindgut carcinoid cell line HC49. In addition we demonstrated that TRP family channels involved in Ca^{2+} transport, temperature sensitivity or taste detection were also expressed in some carcinoid lines. For example, low levels of mRNA for TRPV6, implicated in vitamin D-dependent Ca^{2+} absorption in the human small intestine, were identified in all carcinoid cell lines. In addition, consistent with the work of Mergler [16] we identified TRPM8 and TRPM5 transcripts in BON cells. TRPV2 was identified in BON and CNDT2.5 cells and TRPV1 was detected in H727. TRPM8 and TRPV1 were functionally expressed as indicated by pharmacological activation with menthol or capsaicin, respectively (data not shown).

Functional assessment of non voltage-operated Ca^{2+} channels in carcinoid cell lines

Having identified a variety of SOCE and ROCE candidates, we used fluorescence imaging of Ca^{2+} dynamics to test whether SOCE was activated in the carcinoid cell lines following ER Ca^{2+} store-depletion. In these experiments application of 30 μM cylcopiazonic acid (CPA), a reversible SERCA pump inhibitor, was applied to fura-2 loaded cells in nominal Ca^{2+} containing physiological saline (250 - 500 μM EGTA with no added Ca^{2+}) to deplete intracellular Ca^{2+} stores and activate SOCE pathways. As shown in **Figure 3A**, CPA induced a slow transient rise in [Ca^{2+}]$_i$ attributed to the leak of ER Ca^{2+} and subsequent extrusion from the cytoplasm. Reintroduction of the cells to Ca^{2+} containing bath solution induced a rapid more sustained rise in the fluorescence signal attributed to Ca^{2+} influx through activated SOCE channels. All of the cell lines tested by this method exhibited SOCE and the averaged peak influx induced by store depletion for BON, H727, HC45, HC49 and CNDT2.5, is shown in bar graph in **Figure 3B**. To further demonstrate that the rise in Ca^{2+} reflected influx through a SOCE mechanism we reduced or enhanced the driving force for Ca^{2+} entry by membrane depolarization or increasing [Ca^{2+}]$_o$. An example of a reduction in influx following store depletion is shown in **Figure 3C**. Depolarization by treatment with 50 mM K$^+$ prior to and during restoration of extracellular Ca^{2+} diminished the subsequent influx. The diminished Ca^{2+} entry indicated that VOCCs did not contribute significantly to influx under conditions where prolonged pretreatment with elevated K$^+$ likely inactivated VOCCs. The reduced entry was therefore most likely due to a reduction in the driving force for the entry of Ca^{2+} through SOCCs. In contrast, increasing the extracellular Ca^{2+} concentration to 20 mM enhanced the peak rise in Ca^{2+} influx following store depletion. Because the majority of non-VOCCs are relatively non-selective for Ca^{2+} and conduct monovalent ions, we assessed whether activation of SOCE caused sufficient depolarization to activate VOCC. In these experiments, BON cells were treated with nifedipine to block the dominant HVA VOCC or by vehicle and SOCE influx was assessed and compared. Treatment with the dihydropyridine nifedipine was found to produce only a minor diminishment in influx suggesting that the majority of Ca^{2+} entry induced by store-depletion was through SOCE channels and not through VOCC. As shown in **Figure 3D**, the average amplitudes of SOCE evoked for control or bath solutions containing
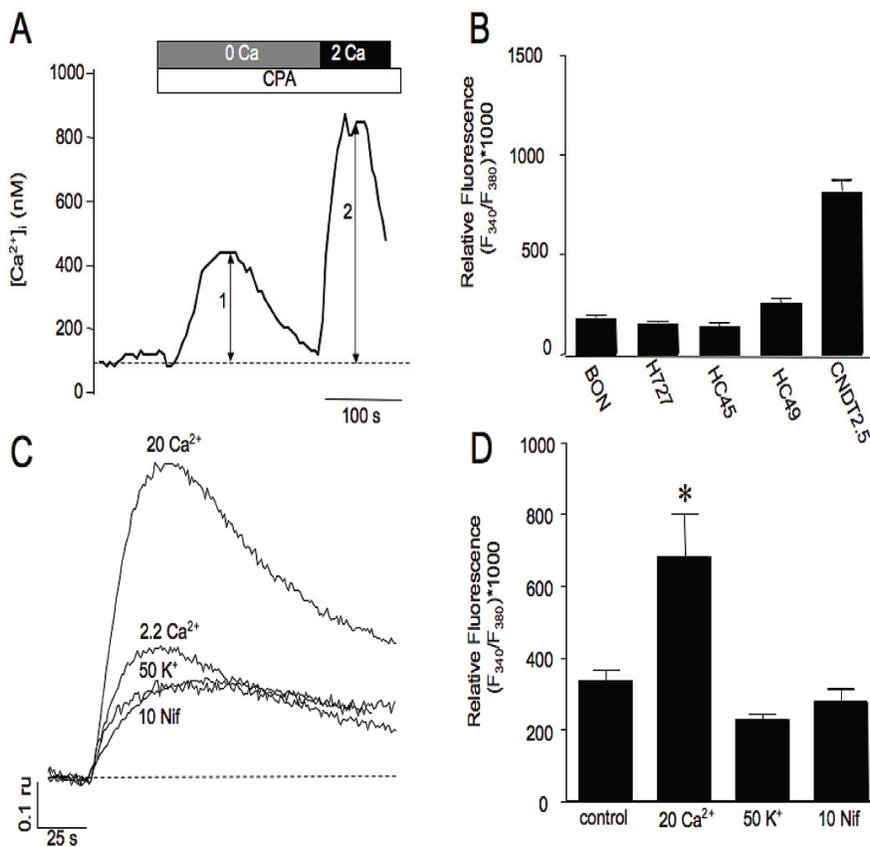
Figure 3. Functional assessment of SOCE in carcinoid cell lines. A. Representative fura-2 trace in a BON cell showing SOCE response (arrow 2) induced by restoration of extracellular Ca^{2+} to bath solution following store-depletion (arrow 1) with CPA in nominal Ca^{2+} containing bath solution. B. Averaged peak amplitudes of SOCE responses. C. Induced influx was augmented by increasing [Ca^{2+}]$_o$ to 20 mM, reduced by membrane depolarization and was not significantly altered by treatment with 10 μM nifedipine (trace 4) compared to control. D. Averaged amplitudes of SOCE activated following treatments indicated in C.

20 mM extracellular Ca^{2+}, 50 mM extracellular K$^+$ or 10 mM Nifedipine was 338±32; 682±121; 227±15; 274±38, respectively (*n* = 7-10; *p* value < 0.05).

A number of inorganic and organic inhibitors of SOCE have been reported that vary in potency and selectivity. For example, lanthanoids, such as La^{3+} and Gd^{3+} or divalent metals such as Ni^{2+} of Cd^{2+} are commonly used inorganic blockers of SOCE. Gd^{3+} is the most effective, specific and best characterized inorganic blocker. Examples of some commonly used organic inhibitors are the putative channel blockers 2-aminoethoxydiphenyl borate (2-APB) and carboxy-amidotriazole (L651582 or CAI) [17-19]. Recently, N-(4-[3,5-bis(trifluoromethyl)-1H-pyrazol-1-yl]phenyl)-4-methyl-1,2,3-thiadiazole-5

-carboxamide (BTP2) has been used as a highly selective blocker of SOCE in lymphocytes [20]. However, most of these inhibitors are thought to act with less than complete specificity and the mechanistic basis of their actions are not well elucidated. Despite this caveat, we chose to compare the actions of Gd^{3+}, 2-APB, CAI and BTP2 on SOCE between the various carcinoid cell lines. As shown in the representative traces in **Figure 4A**, treatment with 1μM Gd^{3+} had no effect on Ca^{2+} release but substantially blocked SOCE in BON cells following reintroduction of Ca^{2+} containing bath solution. 10 μM La^{3+} also blocked SOCE, but only at higher concentrations that caused elevations in [Ca^{2+}]$_i$ that we attributed to non-physiological effects (data not shown). Using this paradigm we found that Gd^{3+} significantly reduced SOCE in most carcinoid
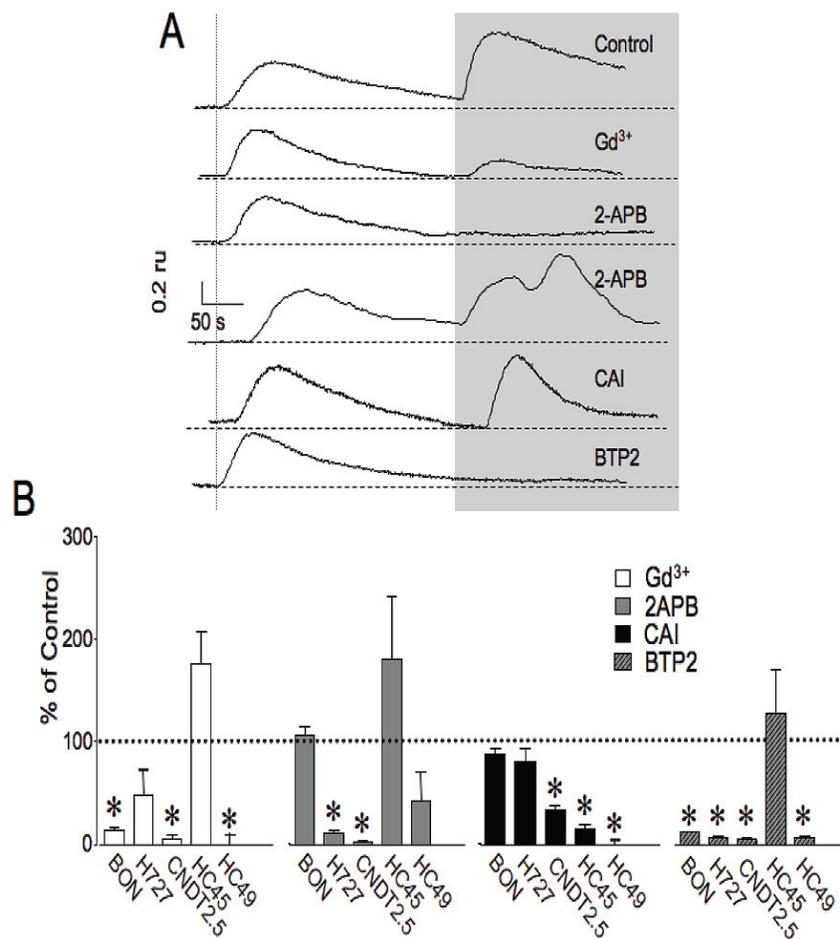
Figure 4. Representative fura-2 traces in BON cells (A) and average peak amplitudes in cell lines tested (B) showing effects of various channel inhibitors on SOCE following restoration of extracellular Ca^{2+} (shaded box). For comparison, traces in A were normalized to Ca^{2+} release peak amplitude. B. Reduction in peak amplitude of SOCE following treatment with inhibitors was compared to control. For BON, H727, CNDT2.5, HC45 AND HC49, the percent reductions in SOCE are listed respectively. Gd^{2+}: 15±3, 49±25, 6±4, 178±32, 0.75±10; 2APB: 107±9.3, 10.4±4, 2.2±6.3, 170±65, 38±30; CAI: 89±6, 81±12, 34±5, 15±5, 0.5±5; BTP2: 12±1.5, 7.4±1.5, 5.5±1, 129±44, 7±3.2; n = 6-104; for significance, p value was < 0.05.

cell lines tested but interestingly did not effectively block Ca^{2+} entry in HC45 cells. The average percent reduction following Gd^{3+} treatment for BON, H727, CNDT2.5 and HC49 is shown in **Figure 4B**. Curiously, Gd^{3+} appeared to enhance Ca^{2+} influx in HC45 cells by nearly two-fold, although these responses were highly variable and did not achieve statistical significance. One possibility for this observation is that Gd^{3+} is known to be an agonist of the calcium-sensing receptor.

Treatment with 100 μM 2-APB generally reduced the magnitude of SOCE in H727,

CNDT2.5 and HC49. However, a more complex response was observed in other cell lines following treatment with 2-APB. 2-APB produced a reduction in SOCE in about half of the BON cells tested but augmented SOCE in the remaining cells. The complex action of 2-APB to activate then inhibit SOCE has previously been reported for other cell types and has been attributed to effects on both STIM and Orai channel paralogues [21]. (Please see discussion.) 2-APB did not significantly diminish Ca^{2+} entry HC45.

In addition, we tested whether the antiproliferative compound CAI that has been shown to in-
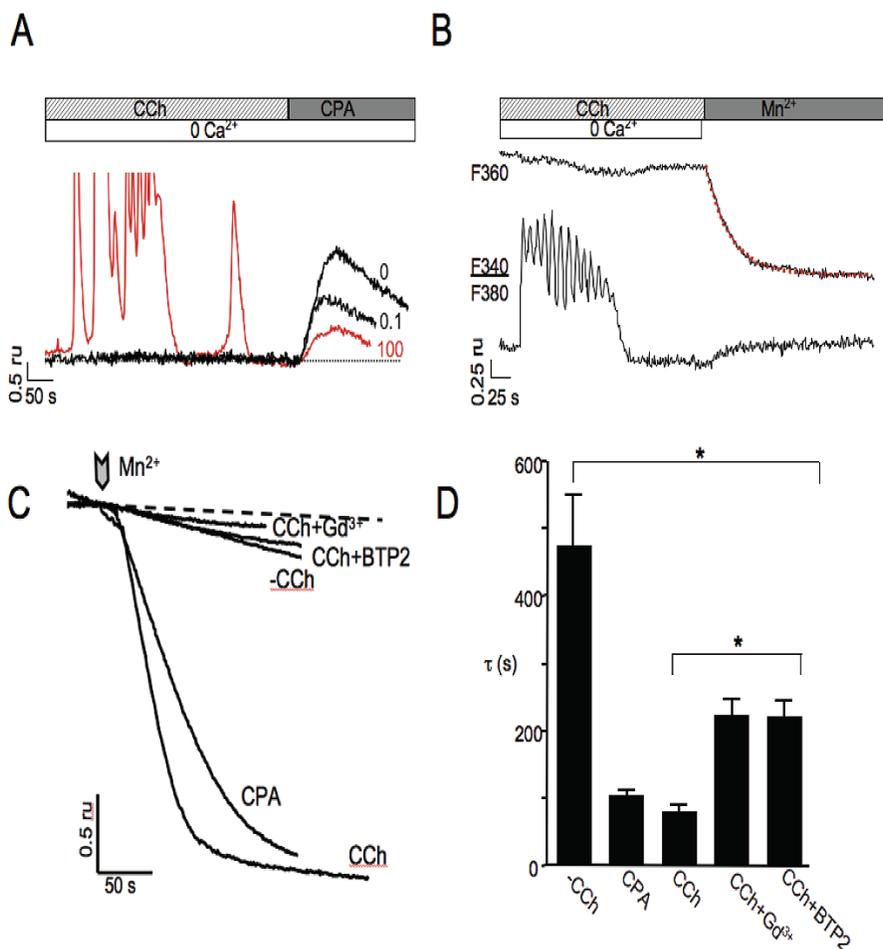
Figure 5. Oscillatory changes in cytosolic Ca^{2+} in response to application of carbachol (CCh). A. Representative traces of Ca^{2+} dynamics induced by CCh in the absence of extracellular Ca^{2+}. 20 μM CPA was applied following CCh evoked response to assess ER Ca^{2+} content. CPA-evoked Ca^{2+} release following treatment with CCh shows a concentration dependent decrease in ER store content. B. A representative trace showing determination of rate of influx by exponential fit (red colored trace) to the slope of Mn^{2+}-induced fura-2 fluorescence quench. C. Representative traces of unstimulated (-CCh) influx and following application of 30 μM CPA or 100 μM CCh in the presence or absence of 1μM Gd^{3+} or BTP2 to measure influx (chevron) determined by Mn^{2+} quench method in fura-2 loaded BON cells. D. Averaged rates (t) of influx under different conditions of activation and block of SOCE.

hibit SOCE in breast cancer and in HEK 293 cells also altered influx in carcinoid cell lines [19, 22]. Pretreatment with 10 μM CAI resulted in diminishment of influx consistent with previous work. The occluding effect was more pronounced for midgut or hindgut cell lines compared to foregut cell lines.

Treatment with 1 μM BTP2 effectively blocked the majority of SOCE in BON, H727, CNDT2.5 and HC49 cells but had no significant effect on Ca^{2+} entry in HC45.

In the aforementioned experiments, SOCE in carcinoid cell lines was activated using the SERCA inhibitor CPA to deplete ER Ca^{2+} stores. Under physiologically relevant conditions influx is typically generated by diminishment of ER stores following robust G-protein coupled receptor activation. Muscarinic receptors are a class of G-protein coupled receptors that are widely expressed in the gastrointestinal tract and have been found to regulate the secretion of several gastrointestinal peptides. For example, muscarinic receptor activation can induce release of

GLP-1 from enteroendocrine L-cells in both cell culture and in the perfused rat ileum [23, 24]. Likewise, acetylcholine has been shown to stimulate secretion through a muscarinic pathway in BON cells [25]. To determine whether muscarinic receptor activation diminished ER Ca^{2+} content sufficiently to activate influx we treated carcinoid cell lines with the acetylcholine receptor agonist carbachol (CCh) in the absence of extracellular Ca^{2+}, monitored the evoked Ca^{2+} dynamics and subsequently applied CPA to assay store content. As shown in **Figure 5A** and **B**, 100 µM CCh application evoked Ca^{2+} oscillations in [Ca^{2+}]$_i$ in BON cells. Accordingly, application of 100 µM CCh (red colored trace), but not 0.1 µM CCh, demonstrated a concentration-dependent reduction in the ER Ca^{2+} store content in the absence of extracellular Ca^{2+} (**Figure 5A**). To assess whether CCh induced Ca^{2+} entry, the Mn^{2+} quench method was used to track influx. Addition of Mn^{2+} to the bath solution under unstimulated conditions (without prior depletion of stores by addition of CCh), following application of 20 µM CPA or following addition of 100 µM CCh alone or in the presence of the SOCE blockers Gd^{3+} or BTP2 produced Mn^{2+} dependent quenching of the fura-2 F$_{360}$ signal. The rates of entry were determined from fits of single exponential lines to the quench of the signals (for example, red colored line in **Figure 5B**) and expressed as the inverse rate constants (t). The t for control cells, 30 µM CPA-treated cells, 100 µM CCh-treated cells, 100 µM CCh-treated cells in the presence of 1 µM Gd^{2+} and CCh-treated cells in the presence of 1µM BTP2 were 473±79 s, 106±9.4 s, 85±11 s, 221±30 s, 223±26; respectively, *n* = 8-57; for significance *p* value was < 0.05.

This indicated that CCh-activated influx was largely blocked by known inhibitors of SOCE (**Figure 5C** and **D**). Similar results were also obtained using H727 cells (data not shown). In contrast, CCh-induced Ca^{2+} signals were not observed in CNDT2.5, HC45 or HC49 cells indicating that these cell lines apparently lacked acetylcholine receptors coupled to Ca^{2+} release.

Taken together, these data are consistent with the expression of functional SOCE channels in carcinoid tumor cell lines. Moreover, the observed differences in the action of pharmacological probes on SOCE between specific cell lines suggests that carcinoid cells arising from differing sites in the gut may express distinct channels and/or pathways of SOCE activation.

Discussion

SOCE in carcinoid cell lines

In contrast to voltage-operated Ca^{2+} entry, Ca^{2+} release in response to growth factors or hormones can induce Ca^{2+} entry by additional pathways termed SOCE and store-independent ROCE. SOCE is distinguished from ROCE in that it is exclusively activated by ER Ca^{2+} store depletion and is not dependent on other signals produced by receptor activation. In this study we demonstrated that SOCE could be induced by ER store depletion with CPA or by GPCR activation in carcinoid cell lines. In the latter, Ca^{2+} entry was dependent on robust muscarinic activation in BON cells, and that entry was blocked by BTP2. Thus we report the novel observation of these additional or alternative Ca^{2+} entry pathways in human carcinoid cancer cell lines. Moreover, these observations are consistent with our identification of STIM1 [26-28]and the pore-forming channel subunits Orai1-Orai3. TRP channel family members that potentially contribute to SOCE and/or ROCE were also identified in carcinoid cell lines.

The best characterized form of SOCE is the Ca^{2+} release activated current (I$_{CRAC}$) of lymphocytes of which the structural determinants include STIM1 (originally identified as a possible tumor suppressor [29]) and pore-forming subunits of Orai1 [12]. Following store depletion STIM1 complexes with SOCE channel proteins to activate Ca^{2+} entry [30, 31].

In addition to STIM1, we identified the three human Orai paralogues in the carcinoid cell lines. These observations are of interest given recent work that demonstrated Orai1 and STIM1 are critical for breast tumor cell migration and metastasis [32]. Generally, we found that the relative mRNA expression levels for these pore-forming subunits was Orai3 > Orai1 > Orai2. The identification of STIM1 and Orai1 largely correlated with our pharmacological profiling of SOCE in carcinoid cell lines. For example, low concentrations of the blockers Gd^{3+} and BTP2 substantially reduced entry in most carcinoid cell lines, consistent with the reported sensitivity of SOCE, but did not reduce entry in the midgut cell line HC45. 2-APB was also ineffective at reducing entry in HC45 even though

Orai1 message was detected in these cell lines. In contrast, 2-APB treatment in BON cells induced a complex response. For example, in some instances it appeared that 2-APB enhanced entry. One interpretation of this observation was that some BON cells express more Orai3 that, in contrast to Orai1, can be activated by 2-APB. Interestingly, the anti-tumor compound CAI was effective at reducing entry in midgut and hindgut carcinoid lines but did not consistently block Ca^{2+} entry in the foregut cell lines. This may point to CAI as a potential compound of interest to target Ca^{2+} entry in ileal carincoids. The observed variability of these treatments may reflect the limited selectivity of these inhibitors, the complexity of channel subunit expression and interactions and/or may indicate that the cell lines used were not clonal. Certainly, without improving the selectivity of blockade using better pharmacological probes, it will be difficult to draw conclusions regarding the identity of channels underlying SOCE in the various carcinoid cell lines. Given this limitation, gene silencing and over expression of dominant negative proteins are likely to be useful approaches to address the roles of Orai1 and STIM1 in these cell lines.

TRP channels in carcinoid cell lines.

TRP channels identified in the carcinoid cell lines in the current study by RT-PCR included TRPC1-7, TRPV6 and TRPM5. In addition application of menthol to BON and H727 cells induced cytosolic Ca^{2+} rises suggesting that these cells expressed TRPM8.. These findings suggested that they might play important roles in encoding sensory information and growth signals in enteroendocrine cells of the gut epithelia or contribute to malignant phenotype in GI cancers.

Some canonical TRP channels (TRPC) have been identified as candidates for SOCE in epithelial cells, and numerous studies have implicated TRPC family members in proliferation and differentiation in a variety of non-transformed and malignant cells [33]. However interactions between TRPC family members are complex and their roles in some forms of SOCE may be tissue specific [34, 35]. TRPC1 is the best-characterized member of the TRPC protein subfamily and has been linked to proliferation, cell migration and apoptosis in intestinal epithelia and in prostate cancer [36-38]. In the current

study, TRPC1 was identified in all of the tested cell lines and its relative expression level was highest for the foregut carcinoid lines and lowest for the midgut carcinoids. The relationship of TRPC1 to SOCE in carcinoid cell lines was not elucidated here, but based on the work of others, it probably does not form functional CRAC channels as over-expression studies do not recapitulate the electrophysiological properties of I$_{CRAC}$. Nevertheless, TRPC1 could still contribute to SOCE in epithelial cells by serving as a component of a store-operated channel. For example, TRPC1 has recently been shown to interact in a complex with Orai1 and STIM [34], but whether endogenous TPRC1-7, Orai1 and STIM1 interact in carcinoid tumor cell lines remains unclear.

Whereas TRPC1 was ubiquitously expressed, other TRP family members were expressed in some cell lines but not in others and specific roles for TRPC channels in enteroendocrine cells or in carcinoid tumors remain largely unknown.

In addition to canonical TRP family members, other TRP subfamily members have been implicated in cancers [33]. For example, message corresponding to TRPV6, known to underlie vitamin D-regulated Ca^{2+} uptake in the intestine, was expressed at relatively low levels in all carcinoid cell lines tested. TRPV6 is highly Ca^{2+} selective and has been shown to potentiate Ca^{2+} dependent cell proliferation [39]. It is aberrantly expressed in a variety of human cancers [40]. In addition to TRPV6, TRPV2 was detected in BON, H727 and CNDT2.5 cells and TRPV1 was detected in H727 cells. TRPM5, which is not Ca^{2+} permeable, and TRPM8 were detected in foregut and bronchial carcinoid cell lines (BON and H727). These channels likely contribute to sensory transduction or secretory function in gut enteroendocrine cells. TRPM7, which is also Ca^{2+} permeable, was not tested in the current study.

The molecular and pharmacological profiling in the present study provides evidence for functional SOCE channels in a set of carcinoid cell lines originating from bronchial epithelium, foregut, midgut and hindgut. Moreover, we demonstrated that ER Ca^{2+} store reduction and subsequent SOCE could be induced by muscarinic acetylcholine receptor activation in BON and H727 cell lines. Because Ca^{2+} entry through non

-voltage operated Ca^{2+} permeable channels has been shown by others to control many important processes in tumorigenesis, these pathways are potential targets for developing new diagnostic tools or anticancer therapies for carcinoid tumors. This work provides a base for the further clarification of the roles Ca^{2+} pathways in enteroendocrine cell biology in health and disease.

Acknowledgements

Please address correspondence to: David Giovannucci, PhD, Department of Neurosciences, College of Medicine/University of Toledo Health Science Campus, Toledo, OH 43614, USA. Tel: 419-383-5004, E-mail: David.Giovannucci@utoledo.edu

References

[1] Berridge MJ, Lipp P and Bootman MD. The versatility and universality of calcium signalling. Nat Rev Mol Cell Biol 2000; 1: 11-21.

[2] Cheng HP, Wei S, Wei LP and Verkhratsky A. Calcium signaling in physiology and pathophysiology. Acta Pharmacol Sin 2006; 27: 767-772.

[3] Lipskaia L and Lompre AM. Alteration in temporal kinetics of Ca2+ signaling and control of growth and proliferation. Biol Cell 2004; 96: 55-68.

[4] Capiod T, Shuba Y, Skryma R and Prevarskaya N. Calcium signalling and cancer cell growth. Subcell Biochem 2007; 45: 405-427.

[5] Ruddat VC, Whitman S, Klein RD, Fischer SM and Holman TR. Evidence for downregulation of calcium signaling proteins in advanced mouse adenocarcinoma. Prostate 2005; 64: 128-138.

[6] Kazerounian S, Pitari GM, Shah FJ, Frick GS, Madesh M, Ruiz-Stewart I, Schulz S, Hajnoczky G and Waldman SA. Proliferative signaling by store-operated calcium channels opposes colon cancer cell cytostasis induced by bacterial enterotoxins. J Pharmacol Exp Ther 2005; 314: 1013-1022.

[7] Koslowski M, Sahin U, Dhaene K, Huber C and Tureci O. MS4A12 is a colon-selective store-operated calcium channel promoting malignant cell processes. Cancer Res 2008; 68: 3458-3466.

[8] Vanden Abeele F, Roudbaraki M, Shuba Y, Skryma R and Prevarskaya N. Store-operated Ca2+ current in prostate cancer epithelial cells. Role of endogenous Ca2+ transporter type 1. J Biol Chem 2003; 278: 15381-15389.

[9] Modlin IM, Oberg K, Chung DC, Jensen RT, de Herder WW, Thakker RV, Caplin M, Delle Fave G, Kaltsas GA, Krenning EP, Moss SF, Nilsson O, Rindi G, Salazar R, Ruszniewski P and Sundin A. Gastroenteropancreatic neuroendocrine tumours. Lancet Oncol 2008; 9: 61-72.

[10] Pinchot SN, Holen K, Sippel RS and Chen H. Carcinoid tumors. Oncologist 2008; 13: 1255-1269.

[11] Yao JC, Hassan M, Phan A, Dagohoy C, Leary C, Mares JE, Abdalla EK, Fleming JB, Vauthey JN, Rashid A and Evans DB. One hundred years after "carcinoid": epidemiology of and prognostic factors for neuroendocrine tumors in 35,825 cases in the United States. J Clin Oncol 2008; 26: 3063-3072.

[12] Smyth JT, Dehaven WI, Jones BF, Mercer JC, Trebak M, Vazquez G and Putney JW, Jr. Emerging perspectives in store-operated Ca2+ entry: roles of Orai, Stim and TRP. Biochim Biophys Acta 2006; 1763: 1147-1160.

[13] Thebault S, Flourakis M, Vanoverberghe K, Vandermoere F, Roudbaraki M, Lehen'kyi V, Slomianny C, Beck B, Mariot P, Bonnal JL, Mauroy B, Shuba Y, Capiod T, Skryma R and Prevarskaya N. Differential role of transient receptor potential channels in Ca2+ entry and proliferation of prostate cancer epithelial cells. Cancer Res 2006; 66: 2038-2047.

[14] Weiss H, Amberger A, Widschwendter M, Margreiter R, Ofner D and Dietl P. Inhibition of store-operated calcium entry contributes to the antiproliferative effect of non-steroidal anti-inflammatory drugs in human colon cancer cells. Int J Cancer 2001; 92: 877-882.

[15] Putney JW, Jr. Recent breakthroughs in the molecular mechanism of capacitative calcium entry (with thoughts on how we got here). Cell Calcium 2007; 42: 103-110.

[16] Mergler S, Strowski MZ, Kaiser S, Plath T, Giesecke Y, Neumann M, Hosokawa H, Kobayashi S, Langrehr J, Neuhaus P, Plockinger U, Wiedenmann B and Grotzinger C. Transient receptor potential channel TRPM8 agonists stimulate calcium influx and neurotensin secretion in neuroendocrine tumor cells. Neuroendocrinology 2007; 85: 81-92.

[17] Bootman MD, Collins TJ, Mackenzie L, Roderick HL, Berridge MJ and Peppiatt CM. 2-aminoethoxydiphenyl borate (2-APB) is a reliable blocker of store-operated Ca2+ entry but an inconsistent inhibitor of InsP3-induced Ca2+ release. FASEB J 2002; 16: 1145-1150.

[18] Munaron L, Antoniotti S, Fiorio Pla A and Lovisolo D. Blocking Ca2+entry: a way to control cell proliferation. Curr Med Chem 2004; 11: 1533-1543.

[19] Yang JL, Qu XJ, Yu Y, Kohn EC and Friedlander ML. Selective sensitivity to carboxyamidotriazole by human tumor cell lines with DNA mismatch repair deficiency. Int J Cancer 2008; 123: 258-

263.

[20] Zitt C, Strauss B, Schwarz EC, Spaeth N, Rast G, Hatzelmann A and Hoth M. Potent inhibition of Ca2+ release-activated Ca2+ channels and T-lymphocyte activation by the pyrazole derivative BTP2. J Biol Chem 2004; 279: 12427-12437.

[21] DeHaven WI, Smyth JT, Boyles RR, Bird GS and Putney JW, Jr. Complex actions of 2-aminoethyldiphenyl borate on store-operated calcium entry. J Biol Chem 2008; 283: 19265-19273.

[22] Mignen O, Brink C, Enfissi A, Nadkarni A, Shuttle-worth TJ, Giovannucci DR and Capiod T. Car-boxyamidotriazole-induced inhibition of mito-chondrial calcium import blocks capacitative calcium entry and cell proliferation in HEK-293 cells. J Cell Sci 2005; 118: 5615-5623.

[23] Anini Y and Brubaker PL. Muscarinic receptors control glucagon-like peptide 1 secretion by hu-man endocrine L cells. Endocrinology 2003; 144: 3244-3250.

[24] Anini Y, Hansotia T and Brubaker PL. Muscarinic receptors control postprandial release of gluca-gon-like peptide-1: in vivo and in vitro studies in rats. Endocrinology 2002; 143: 2420-2426.

[25] Tran VS, Marion-Audibert AM, Karatekin E, Huet S, Cribier S, Guillaumie K, Chapuis C, Desnos C, Darchen F and Henry JP. Serotonin secretion by human carcinoid BON cells. Ann N Y Acad Sci 2004; 1014: 179-188.

[26] Roos J, DiGregorio PJ, Yeromin AV, Ohlsen K, Lioudyno M, Zhang S, Safrina O, Kozak JA, Wag-ner SL, Cahalan MD, Velicelebi G and Stauder-man KA. STIM1, an essential and conserved component of store-operated Ca2+ channel function. J Cell Biol 2005; 169: 435-445.

[27] Liou J, Kim ML, Heo WD, Jones JT, Myers JW, Ferrell JE, Jr. and Meyer T. STIM is a Ca2+ sen-sor essential for Ca2+-store-depletion-triggered Ca2+ influx. Curr Biol 2005; 15: 1235-1241.

[28] Zhang SL, Yeromin AV, Zhang XH, Yu Y, Safrina O, Penna A, Roos J, Stauderman KA and Cahalan MD. Genome-wide RNAi screen of Ca(2+) influx identifies genes that regulate Ca(2+) release-activated Ca(2+) channel activity. Proc Natl Acad Sci U S A 2006; 103: 9357-9362.

[29] Sabbioni S, Veronese A, Trubia M, Taramelli R, Barbanti-Brodano G, Croce CM and Negrini M. Exon structure and promoter identification of STIM1 (alias GOK), a human gene causing growth arrest of the human tumor cell lines G401 and RD. Cytogenet Cell Genet 1999; 86: 214-218.

[30] Zhang SL, Yu Y, Roos J, Kozak JA, Deerinck TJ, Ellisman MH, Stauderman KA and Cahalan MD. STIM1 is a Ca2+ sensor that activates CRAC channels and migrates from the Ca2+ store to the plasma membrane. Nature 2005; 437: 902-905.

[31] Liao Y, Erxleben C, Yildirim E, Abramowitz J, Arm-strong DL and Birnbaumer L. Orai proteins inter-act with TRPC channels and confer responsive-ness to store depletion. Proc Natl Acad Sci U S A 2007; 104: 4682-4687.

[32] Yang S, Zhang JJ and Huang XY. Orai1 and STIM1 are critical for breast tumor cell migration and metastasis. Cancer Cell 2009; 15: 124-134.

[33] Prevarskaya N, Zhang L and Barritt G. TRP chan-nels in cancer. Biochim Biophys Acta 2007; 1772: 937-946.

[34] Ong HL, Cheng KT, Liu X, Bandyopadhyay BC, Paria BC, Soboloff J, Pani B, Gwack Y, Srikanth S, Singh BB, Gill DL and Ambudkar IS. Dynamic assembly of TRPC1-STIM1-Orai1 ternary complex is involved in store-operated calcium influx. Evi-dence for similarities in store-operated and cal-cium release-activated calcium channel compo-nents. J Biol Chem 2007; 282: 9105-9116.

[35] Worley PF, Zeng W, Huang GN, Yuan JP, Kim JY, Lee MG and Muallem S. TRPC channels as STIM1-regulated store-operated channels. Cell Calcium 2007; 42: 205-211.

[36] Marasa BS, Rao JN, Zou T, Liu L, Keledjian KM, Zhang AH, Xiao L, Chen J, Turner DJ and Wang JY. Induced TRPC1 expression sensitizes intesti-nal epithelial cells to apoptosis by inhibiting NF-kappaB activation through Ca2+ influx. Biochem J 2006; 397: 77-87.

[37] Marasa BS, Xiao L, Rao JN, Zou T, Liu L, Wang J, Bellavance E, Turner DJ and Wang JY. Induced TRPC1 expression increases protein phos-phatase 2A sensitizing intestinal epithelial cells to apoptosis through inhibition of NF-kappaB activation. Am J Physiol Cell Physiol 2008; 294: C1277-1287.

[38] Rao JN, Platoshyn O, Golovina VA, Liu L, Zou T, Marasa BS, Turner DJ, Yuan JX and Wang JY. TRPC1 functions as a store-operated Ca2+ chan-nel in intestinal epithelial cells and regulates early mucosal restitution after wounding. Am J Physiol Gastrointest Liver Physiol 2006; 290: G782-792.

[39] Schwarz EC, Wissenbach U, Niemeyer BA, Strauss B, Philipp SE, Flockerzi V and Hoth M. TRPV6 potentiates calcium-dependent cell prolif-eration. Cell Calcium 2006; 39: 163-173.

[40] Zhuang L, Peng JB, Tou L, Takanaga H, Adam RM, Hediger MA and Freeman MR. Calcium-selective ion channel, CaT1, is apically localized in gastrointestinal tract epithelia and is aber-rantly expressed in human malignancies. Lab Invest 2002; 82: 1755-1764.